Signature OH Absorption Spectrum from Cluster Models of Solvation: A Solvent-to-Solute Charge Transfer State

Ming-Kang Tsai,[†] Karol Kowalski,[‡] Marat Valiev,[‡] and Michel Dupuis*,[†]

Chemical & Materials Sciences Division, Pacific Northwest National Laboratory, K1-83, P.O. 999, Richland, Washington 99352, William R. Wiley Environmental Molecular Sciences Laboratory, Pacific Northwest National Laboratory, K8-91, P.O. 999, Richland, Washington 99352

Ab initio electronic structure theory calculations on cluster models support the characterization of the signature absorption spectrum of a solvated hydroxyl OH radical as a solvent-to-solute charge transfer state modulated by the hydrogen-bonding environment. Vertical excited states in $OH(H_2O)_n$ clusters ($n = 0$–7, 16) calculated at the TDDFT level of theory (with companion calculations at the EOM-CCSD level of theory for $n \leq 7$) show an intense band in the region of ~250 nm. The calculations suggest that the intensity of the solvent-to-solute charge transfer transition depends strongly on a favorable alignment of the donor and acceptor molecular orbitals, as observed in one ($n = 16$) cluster. In the other (smaller) clusters, the transitions in this region were found to be weak as the clusters do not offer the necessary favorable alignment of orbitals. The present findings are consistent with the experimentally observed absorption at 230 nm that has been assigned to a solvent-to-solute charge transfer and provide insight into the electronic states and orbitals that give rise to the intensity of the band.

I. Introduction

Water radiolysis has been extensively studied in recent decades.[1] Reactions of radicals created by water radiolysis are of importance in nuclear reactors, storage of transuranic and high-level mixed wastes, biological effects of radiation therapy, and industrial materials processes. The primary product of water radiolysis is the OH radical.[2,3] The adsorption spectrum of the OH radical in aqueous solution and in supercritical water that is used as a signature of its lifetime and of its reaction dynamics[4] has been a subject of interest over the last 30 years,[5] but there remains uncertainties and discrepancies about the assignment of the signature absorption band. The most recent measurements by Janik et al. show a weak absorption band around 310 nm (4.00 eV) for temperatures above 300 °C in supercritical conditions.[6] This absorption is not observed at room temperature and is assigned to the $^2\Sigma^+ \leftarrow {}^2\Pi$ transition of a "free" OH radical. The absorption intensity is stronger in the range of 320 nm (3.88 eV) to 230 nm (5.39 eV). The absorption intensity at 230 nm decreases with increasing temperature 30–350 °C. These authors describe this 230 nm absorption band as a charge transfer transition from the solvent water molecules to the OH moiety that is modulated by the hydrogen bond network of the environment. In contrast, Nielsen et al. describe the transition near 230 nm as essentially a $^2\Sigma^+ \leftarrow {}^2\Pi$ transition in the OH moiety that is perturbed by various situations of hydrogen bonding of the radical with the solvent.[7]

To date, a theoretical characterization of the signature absorption spectrum of the OH radical in solvated environments has not been reported. Such a characterization is the focus of this work. Previous theoretical studies of the electronic spectrum were limited to calculations on the free OH radical and on a

* Corresponding author. E-mail: michel.dupuis@pnl.gov.
† Chemical & Materials Sciences Division.
‡ William R. Wiley Environmental Molecular Sciences Laboratory.

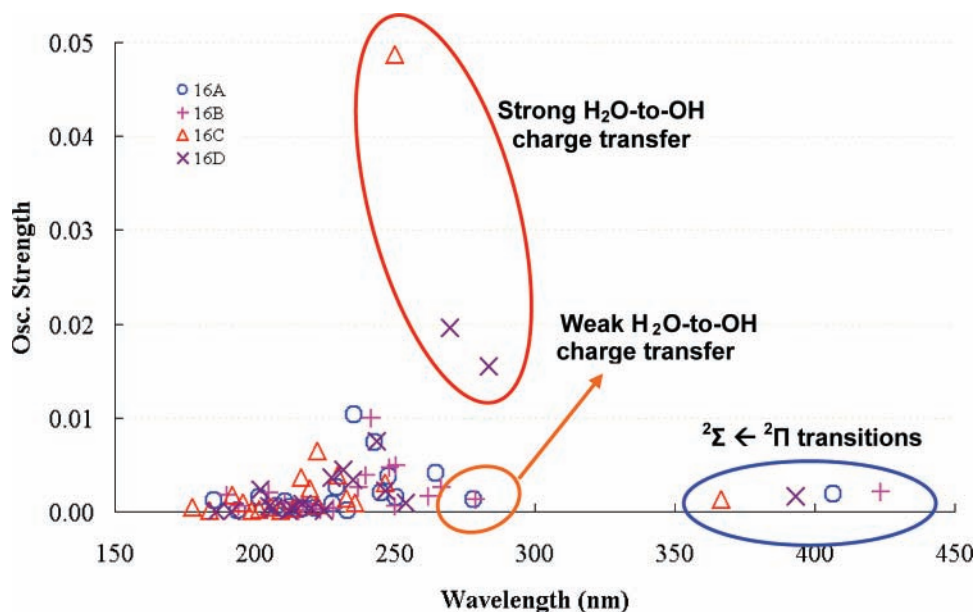**TABLE 1: Vertical Excitation Energies (in eV) of the First Three Excited States of the $OH(H_2O)_n$ Clusters ($n = 0$–7,16) at the TDDFT(MPW1K)/6-31++G** Level of Theory**

n	Ex1	Os1[a]	Ex2	Os2	Ex3	Os3
0	0.23	0.00	4.38	3.12	7.77	8.85
1	0.25	0.00	3.97	2.76	7.41	3.18
2	0.39	0.00	3.71	2.21	6.10	2.43
3	0.45	0.01	3.47	1.80	5.96	3.02
4	0.45	0.01	3.41	1.59	5.94	1.66
5	0.44	0.00	3.42	1.58	5.92	4.76
6	0.39	0.01	3.33	1.64	5.90	1.34
7	0.46	0.02	3.11	2.27	5.53	10.88
16A	0.59	0.01	3.05	1.91	4.46	1.29
16B	0.54	0.03	2.93	2.08	4.44	2.79
16C	0.70	0.04	3.38	1.27	4.96	48.66
16D	0.63	0.03	3.16	1.63	4.38	15.48

^{a} Os denotes oscillator strength $\times 10^3$ (unitless).

TABLE 2: Vertical Excitation Energies (in eV) of the First Three Excited States of the $OH(H_2O)_n$ Clusters ($n = 0$–7) at the EOM-CCSD/6-31++G Level of Theory**

n	Ex1	Os1[a]	Ex2	Os2	Ex3	Os3
0	0.01	0.00	4.24	2.77	7.43	9.27
1	0.03	0.00	3.89	2.64	7.37	0.00[b]
2	0.15	0.00	3.74	2.23	6.89	2.75
3	0.20	0.00	3.56	1.86	6.62	2.52
4	0.20		3.50			
5	0.20		3.50			
6	0.15		3.41			
7	0.22		3.28			

^{a} Os denotes oscillator strength $\times 10^3$ (unitless). ^{b} EOM-CCSD predicts the third excitation of $OH(H_2O)$ as $\sigma^* \leftarrow \pi$ of water.

$OH(H_2O)$ complex using various advanced electronic structure methods.[8,9] These studies focused only on the lowest vertical and adiabatic excitation energies of each symmetry; in particular, they did not address the characterization of solvent-to-solute transitions. Calculations at the couple cluster level of theory

OH Absorption Spectrum from Cluster Models

J. Phys. Chem. A, Vol. 111, No. 42, 2007 **10479**

Figure 1. Excitation energies of the four OH(H$_2$O)$_{16}$ clusters calculated at the TDDFT level of theory (the first 20 excitations are reported for each cluster). The first excitations are outside the range of wavelength. The second excitations are shown in the blue circle. The orange circle denotes the weak Ex3 excitations for the 16A and 16B clusters. The red circle includes the strong Ex3 excitation for cluster 16C and the strong Ex3 and Ex4 excitations for cluster 16D.

(with iterative treatment of triple excitations (CC3) using the aug-cc-pVTZ basis set) showed that the $^2\Sigma^+ \leftarrow {}^2\Pi$ transition of the free OH radical is shifted to the red by 0.37 eV when the OH radical is hydrated by a single water molecule.[10] The adiabatic excitation energy for the $^2A' \leftarrow {}^2A'$ transition in the OH(H$_2$O) complex was also found to be shifted to the red by nearly 1.0 eV.

In the present study, we report extensive ab initio electronic structure calculations on the "free" OH radical and on hydrated clusters of selected sizes OH(H$_2$O)$_n$ (n =1−7, 16) as mimics of aqueous solvation. We analyze the variations in vertical excitation energies as a function of the degree of hydration and characterize the absorption bands of the OH radical in these hydrated environments. The findings described below are consistent with the experimentally observed absorption band at 230 nm, being indeed assigned to a solvent-to-solute charge transfer, and provide a detailed analysis of the electronic states and orbitals that give rise to the intensity of the transition. The computational methods are presented in Section II. The results of the calculations are presented in Section III. The conclusions are summarized in Section IV.

II. Computational Methods

The OH radical was solvated by water clusters (H$_2$O)$_n$ (n = 1−7, 16). The geometries of OH(H$_2$O)$_n$ clusters were optimized at the density functional (DFT) level of theory using the MPW1K functional[11] and the 6-31++G** basis set,[12] which includes polarization and diffuse functions. The latter are especially important because we are interested in higher excited states, albeit the excited states considered here are not expected to have such a diffuse character that more diffuse functions might be required. Excited states were calculated using the time-dependent DFT(TDDFT)/6-31++G** level of theory with the Tamm−Dancoff approximation and frozen core orbitals.[13] The TDDFT calculations were accompanied by calculations at the spin-unrestricted equation-of-motion coupled cluster with singles and doubles (EOM-CCSD)/6-31++G** level of theory at MP2/6-31++G** optimized geometries of the clusters. Indeed, MP2 geometries are expected to be very similar to CCSD geometries,

and in this manner, we avoided that the EOM-CCSD excitation energies would be biased by the DFT geometries. With increasingly larger clusters, the size of the basis set of the clusters increases, giving rise to an error analogous to a "basis set superposition error" whereby calculations on the smaller clusters ought to have included ghost functions from the missing water molecules for consistency. We did not account for such an inconsistency. We feel that it is unlikely that the extra functions, when added to the smaller clusters, would change drastically the excitations energies.

Only the global minimum energy structures were considered for the n = 1−7 clusters.[14] Four structures for n = 16 were generated from four initial geometries derived from the global minimum of the (H$_2$O)$_{17}$ cluster by removing one hydrogen atom from the core water molecule (fully solvated) and rearranging the surrounding water molecules to form four distinct hydrogen-bonding patterns. These structures were subsequently fully optimized at the DFT(MPW1K)/6-31++G** level of theory. The coordinates of the optimized geometries are included as Supporting Information. These four (n = 16) clusters, denoted 16A−D, are close in energy (16A, 16B, and 16C are 0.014, 0.012, and 0.036 eV higher in energy than 16C, respectively) and differ only through their hydrogen-bonding patterns. The core OH radical acts as a donor in one hydrogen bond and as an acceptor in two hydrogen bonds in 16A and 16C, and it acts as a donor in one hydrogen bond and an acceptor in three hydrogen bonds in 16B and 16D. Note that, among the four (n = 16) clusters, the preferential stability of 16C over the other configurations is slightly more than $^1/_2$ kT at room temperature so that 16C is expected to be a dominant configuration albeit lower energy clusters may exit. The four starting configurations were selected simply because they correspond to four obvious and distinct bonding arrangements. No exhaustive search and sampling of phase space was carried out in light of the computational cost of the TDDFT calculations on (n = 16) clusters. The various cluster sizes (n = 1−7, 16) were selected because they represent models with increasing numbers of hydrogen bonds, from a "free" OH radical to a "fully solvated" radical, and because they can be considered as relevant models
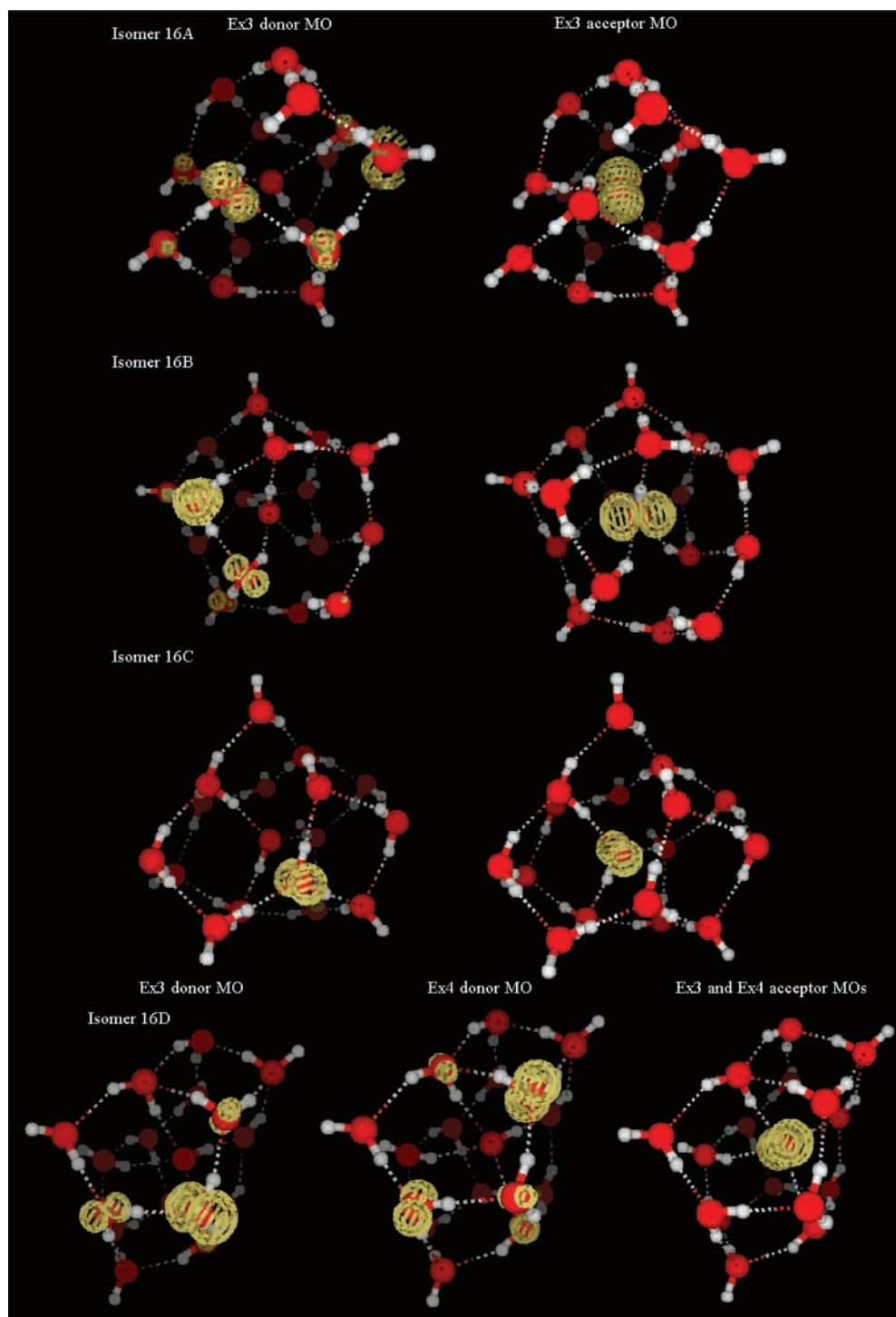
Figure 2. Dominant donor and acceptor molecular orbitals in the Ex3 excitation for the four $OH(H_2O)_{16}$ clusters and the dominant donor molecular orbital in the Ex4 excitation for the 16D isomer. The isodensity surface corresponds to a value of 0.1 au.

of solvation in supercritical water where density is nonuniform. Indeed, as temperature increases toward critical, water gains a clusterlike structure with prevalence of dimers and trimers.[15] The calculations were carried out with the NWChem 5.0 computational chemistry package.[16]

III. Results

The TDDFT level of theory is in good agreement with the higher level EOM-CCSD level of theory used here and the much higher CC3 level of theory used in previously reported calculations on the $n = 0$ and 1 systems.[8,9] The vertical excitation energies for $n \leq 7$ clusters calculated at the TDDFT level of

theory are reported in Table 1, and the EOM-CCSD results are reported in Table 2. It can be seen that the differences in excitation energies between the two methods are less than 0.3 eV for the first (low lying) Ex1, second Ex2, and third Ex3 excited states, except for Ex3 with $n = 2,3$ where the differences are larger, up to 0.7 eV. We believe that the discrepancy between the two methods is small enough to draw reliable conclusions for the smaller and larger clusters. With this in mind, it is noteworthy that there is good agreement between the two methods in the trends (decreasing excitation energies) as a function of the level of hydration. We note also that previous ab initio calculations reported 4.13 eV (300 nm) for the vertical

OH Absorption Spectrum from Cluster Models

J. Phys. Chem. A, Vol. 111, No. 42, 2007 **10481**

$^2\Sigma(\sigma\pi^4) \leftarrow {}^2\Pi(\sigma^2\pi^3)$ transition of the free OH radical and 3.77 eV (329 nm) for the vertical $^2A' \leftarrow {}^2A'$ transition of the OH(H2O) complex at the EOM-CCSD level of theory on the CCSD(T)/aug-cc-pVTZ optimized geometries with the oscillator strengths at 1.75×10^{-3} and 1.55×10^{-3}.[9] In the notation above, σ denotes the OH σ bond orbital and π denotes the $2p\pi$ atomic-like orbital on the oxygen atom of the radical. In the present study (using a somewhat smaller basis set), the corresponding vertical excitation energies were calculated to be 4.24 eV (292 nm) and 3.89 eV (319 nm) with the oscillator strengths of 2.77×10^{-3} and 2.64×10^{-3} at the EOM-CCSD level of theory at MP2/6-31++G** optimized geometries, respectively, similar to the results of Schofield and Kjaergaard.[8] In a hydrated environment, the $^2\Pi$ ground state of the OH radical loses the degenerate character of the π radical, giving rise to a ground state and a low-lying excited state. The low-lying first excitation (Ex1) corresponds to the transition between these two states, with an electron promoted from the doubly occupied $O(2p\pi)$ orbital of the OH radical to the singly occupied π molecular orbital (SOMO). Note that, for $n = 0$, Ex1 should be exactly zero, if it were not for the broken spatial symmetry of the Hartree–Fock and Kohn–Sham determinant used as reference in the excited-state calculations. The second excitation (Ex2) of the free OH radical corresponds to the $\pi \leftarrow \sigma$ excitation from the OH σ bond to the π singly occupied molecular orbital (SOMO) and is calculated to be in good accord with the experimentally observed band at 308 nm (4.03 eV) in the gas phase.[17] It is seen that Ex2 shifts to the red as a function of the degree of hydration for $n = 1–7$, 16. The strength of solvation can be seen in the OH bond length of the OH radical as the bond length increases from 0.974 to 1.012 Å in the largest (more hydrated) cluster like 16B.

For all the clusters studied here, starting with OH(H2O), the third excited state Ex3 is found to correspond to a charge transfer from a solvent orbital to the solute radical orbital. We ascribe this excited state as a solvent-to-solute charge transfer for $n = 1–7$, 16. Ex3 exhibits a dramatic red-shift from 7.41 eV (167 nm) for $n = 1$ down to ~4.4 eV (282 nm) for $n = 16$ at the TDDFT level of theory. We note that the oscillator strength of Ex3 in cluster 16C is significantly stronger than in any of the other clusters, with clusters $n = 7$ and 16D having medium intensity. Thus the oscillator strength is strongly dependent on the solvent structure (the hydrogen-bonding environment around the radical), as further discussed below. The magnitude of the oscillator strength of Ex3 for cluster 16C is more than 1 order of magnitude more intense than that of Ex2 in the "free" OH radical.

The energy and oscillator strength distribution of the first 20 vertical excited states calculated at the TDDFT level of theory for the four OH(H2O)16 clusters are displayed in Figure 1. Ex3 of cluster 16C and Ex3 and Ex4 of cluster 16D stand out for their intensities among all the calculated excited states between 150 and 450 nm. The MOs involved in the dominant configuration for Ex3 in all four $n = 16$ clusters and Ex4 in cluster 16D are shown in Figure 2. The donor and acceptor MOs for Ex3 of cluster 16C are well localized and in good coaxial alignment that gives rise to an oscillator strength of 48.66×10^{-3}, with the oxygen–oxygen distance of 2.75 Å. For cluster 16D, the MOs corresponding to the dominant configurations of Ex3 and Ex4 (another solvent-to-solute charge transfer transition) involve multiple solvent molecules. The delocalized character of the donor orbital decreases the magnitude of the overlap with the acceptor orbital of the OH radical. The oxygen–oxygen distances between the strongest electron donor

solvent molecule (the water molecule with the largest lobe in the picture) and the radical are 3.44 and 2.91 Å, respectively. The delocalized character and increased O–O distances are consistent with the calculated oscillator strengths of Ex3 and Ex4 in cluster 16D being smaller that in cluster 16C. The oscillator strengths of Ex3 in clusters 16A and 16B are significantly smaller than that in cluster 16C because of the poor alignment between donor and acceptor orbitals. Similarly for all the smaller clusters $n = 1–7$, the orbital alignments are unfavorable for large oscillator strengths.

To assess the effect of the hydrogen-bonding environment on the electronic transition in cluster 16C, we carried out a model calculation in which we included only the OH radical and the one donor water molecule in the cluster that comprises the largest contribution to the Ex3 state. The TDDFT calculated excitation energy for this model dimer yielded an excitation of 5.42 eV (237 nm) and an oscillator strength of 64.20×10^{-3} compared to 4.96 eV (250 nm) for the full cluster 16C, a shift of 0.46 eV. Thus the rest of the water molecules in 16C are causing a lowering of the Ex3 excitation energy and a decrease in the oscillator strength compared to the model dimer.

Under high-temperature (e.g., 350 °C) and supercritical conditions as in the experiment by Janik et al., it is expected that smaller clusters are the more relevant models of solvation, while larger clusters are more relevant to low-temperature conditions because the population of smaller clusters increases at higher temperature. This observation is consistent with the low-intensity band at 310 nm being assigned by these authors to "free" OH radicals. Increased population of small clusters, for example $n = 0–7$, is consistent with the intensity of the signature absorption band at 230 nm decreasing with increased temperature because the smaller clusters have been calculated to have small Ex3 oscillator strength.

IV. Conclusions

We reported ab initio electronic structure calculations that aimed to elucidate the nature of the excited states of the OH radical in various water clusters as models of aqueous solvation relevant to supercritical conditions. The third excitation in all the clusters OH(H2O)$_n$ ($n = 1–7$, 16) was found to involve a solvent-to-solute charge transfer transition, in the region of 250 nm (calculated), close to the region of experimental observation of 230 nm. This was particularly the case for cluster 16C that was found to have a large solvent-to-solute transition oscillator strength. The donor and acceptor orbitals in that excitation were found to have favorable near-coaxial alignment. Orbital alignment and solvent–solute oxygen–oxygen distances were shown to be important factors affecting the intensity of the solvent-to-solute charge transfer excitation absorption.

Dynamics, temperature, and pressure were not explicitly accounted for in the present investigation. Nevertheless the series of clusters used here allowed us to infer on the observed temperature dependence of the transition in the 230 nm region. The temperature effects were indirectly addressed by varying the size of OH(H2O)$_n$ clusters. The larger clusters studied here depict a fully solvated OH radical that is relevant to low-temperature conditions, with one structure exhibiting a large oscillator strength for the solvent-to-solute transition due to favorable structure and orbital features. In other structures and with unfavorable orbital alignment, the oscillator strength for such a transition is small. The smaller clusters that are likely to be relevant at high temperature in supercritical conditions all display small oscillator strengths. These findings are consistent with the experimentally observed attenuation of the OH

signature absorption transition at higher temperature. Finally, we note that the Ex3 transition energy increases with decreasing cluster size. Accordingly, these calculations suggest that the maximum of the absorption peak in the region of 230 nm shifts to the blue with increasing temperature.

Supporting Information Available: Cartesian coordinates of the optimized $OH(H_2O)_n$, $n = 0-7$ and 16, clusters at MPW1K/6-31++G** calculations. This material is available free of charge via the Internet at http://pubs.acs.org.

References and Notes

(1) Jonah, C. D. *Radiat. Res.* **1995**, *144*, 141.
(2) Draganic, I. G.; Draganic, Z. D. *The Radiation Chemistry of Water*; Academic Press: New York 1971.
(3) Gonzalez, M. G.; Pliveros, E.; Worner, M.; Braun, A. M. *J. Photochem. Photobiol., C* **2004**, *5*, 225.
(4) Elliot, A. J. *Rate Constants and G-Values for the Simulation of the Radiolysis of Light Water over the Range 0−300 °C.*; Technical REport AECL-11073; Atomic Energy of Canada Ltd: Chalk River, Ontario; 1994.
(5) Hermann, H. *Chem. Rev.* **2003**, *103*, 4691.
(6) Janik, I.; Bartels, D. M.; Jonah, C. D. *J. Phys. Chem. A* **2007**, *111*, 1835.
(7) Nielsen, S. O.; Michael, B. D.; Hart, E. J. *J. Phys. Chem.* **1976**, *80*, 2482.
(8) Schofield, D. P.; Kjaergaard, H. G. *J. Chem. Phys.* **2004**, *120*, 6930.
(9) Crawford, T. D.; Abrams, L.; King, R. A.; Lane, J. R.; Schofield, D. P.; Kjaergaard, H. G. *J. Chem. Phys.* **2006**, *125*, 204302.
(10) Smith, C. E.; King, R. A.; Crawford, T. D. *J. Chem. Phys.* **2005**, *122*, 054110.
(11) Lynch, B. J.; Fast, P. L.; Harris, M.; Truhlar, D. G. *J. Phys. Chem. A* **2000**, *104*, 4811.
(12) Hehre, W. J.; Ditchfield, R.; Pople, J. A. *J. Chem. Phys.* **1972**, *56*, 2257.
(13) Hirata, S.; Head-Gordon, M. *Chem. Phys. Lett* **1999**, *314*, 291.
(14) Du, S.; J, F.; Schenter, G.; Iordanov, T.; Garrett, B.; Dupuis, M.; Li, J. *J. Chem. Phys.* **2006**, *124*, 224318.
(15) Oparin, R. D.; Fedotova, M. V. *Russ. J. Gen. Chem.* **2007**, *77*, 17.
(16) Bylaska, E. J.; de Jong, W. A.; Kowalski, K.; Straatsma, T. P.; Valiev, M.; Wang, D.; Aprà, E.; Windus, T. L.; Hirata, S.; Hackler, M. T.; Zhao, Y.; Fan, P.-D.; Harrison, R. J.; Dupuis, M.; Smith, D. M. A.; Nieplocha, J.; Tipparaju, V.; Krishnan, M.; Auer, A. A.; Nooijen, M.; Brown, E.; Cisneros, G.; Fann, G. I.; Früchtl, H.; Garza, J.; Hirao, K.; Kendall, R.; Nichols, J. A.; Tsemekhman, K.; Wolinski, K.; Anchell, J.; Bernholdt, D.; Borowski, P.; Clark, T.; Clerc, D.; Dachsel, H.; Deegan, M.; Dyall, K.; Elwood, D.; Glendening, E.; Gutowski, M.; Hess, A.; Jaffe, J.; Johnson, B.; Ju, J.; Kobayashi, R.; Kutteh, R.; Lin, Z.; Littlefield, R.; Long, X.; Meng, B.; Nakajima, T.; Niu, S.; Pollack, L.; Rosing, M.; Sandrone, G.; Stave, M.; Taylor, H.; Thomas, G.; van Lenthe, J.; Wong, A.; Zhang, Z. *NWChem*, revision 5.0; Pacific Northwest National Laboratory: Richland, Washington, 2006.
(17) Minschwaner, K.; Canty, T.; Burnett, C. *J. Atmos. Sol.-Terr. Phys.* **2003**, *65*, 335.